Supporting information

Facile synthesis of a Bi_2MoO_6 nanosheets/TiO_2 nanotube arrays composite by the solvothermal method and its application for high-performance supercapacitor

Jiang Wen, Shupei Sun, Bo Zhang, Nianfeng Shi, Xiaoming Liao*, Guangfu Yin, Zhongbing Huang, Xianchun Chen, Ximing Pu

College of Materials Science and Engineering, Sichuan University, Chengdu, Sichuan 610065, China

Table S1. Experimental conditions of the prepared samples.

Samples	[Precursors] (mmol) [a]		Temperature	Time
	$Bi(NO_3)_3 \cdot 5H_2O$	$Na_2MoO_4 \cdot 2H_2O$	(°C)	(h)
BMO/TNT-1	1.0	0.5	160	4
BMO/TNT-2	1.0	0.5	160	8
BMO/TNT-3	1.0	0.5	160	12
BMO/TNT-4	1.0	0.5	160	16
BMO/TNT-5	0.5	0.25	160	12
BMO/TNT-6	2.0	1.0	160	12
BMO/TNT-7	4.0	2.0	160	12
BMO/TNT-8	1.0	0.5	140	12
BMO/TNT-9	1.0	0.5	180	12
BMO/TNT-10	1.0	0.5	200	12
Bi_2MoO_6/Ti	1.0	0.5	160	12

[a] 50 ml ethylene glycol add to all the samples as precursor.

To study the effect of precursor amounts on compositions and morphologies of the Bi_2MoO_6/TNTs, different amount of $Bi(NO_3)_3 \cdot 5H_2O$ and $Na_2MoO_4 \cdot 2H_2O$ (molar ratio 2:1) were dissolved in 50 mL of ethylene glycol. The Bi_2MoO_6/TNTs prepared at 160 ℃ for 12 h with different amount of $Na_2MoO_4 \cdot 2H_2O$: 0.25 mmol, 1.0 mmol and 2.0 mmol were referred as BMO/TNT-5, BMO/TNT-6 and BMO/TNT-7 , respectively.

* Corresponding author. Fax: +86 28 85413003. E-mail: sherman_xm@163.com (X.M. Liao).

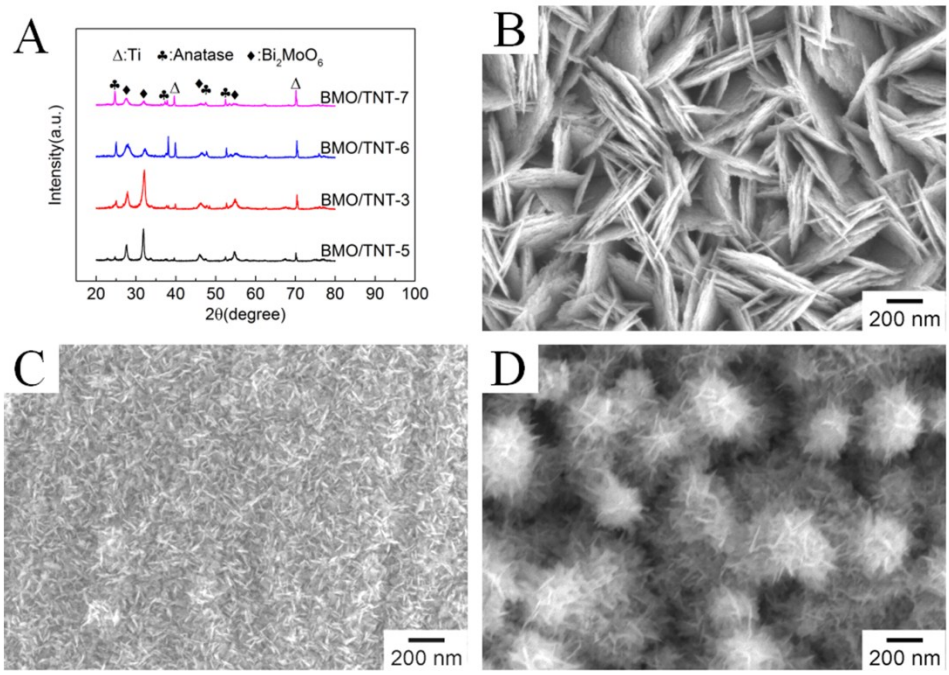

Fig.S1 XRD patterns of the samples BMO/TNT-5, BMO/TNT-3, BMO/TNT-6 and BMO/TNT-7 (A). SEM images of BMO/TNT-5 (B), BMO/TNT-6 (C), BMO/TNT-7 (D).

From Fig. S1A, we can see all samples are composed of Ti, anatase TiO_2 and Bi_2MoO_6. As can be observed, when the amount of $Na_2MoO_4 \cdot 2H_2O$ is 0.25 mmol, the nanosheets are uniformly distributed across the surface without aggregation (Fig. S1B). The surface morphology of BMO/TNT-5 presents thinner nanosheets structure than that of BMO/TNT-3. When the amount is increased to 1.0 mmol , a number of Bi_2MoO_6 nanoparticles, instead of nanosheets, grow on the surface of the TNTs. In this case, the TNTs provide a great deal of sites for the adsorption of metal ions (Bi^{3+}, Mo^{6+}) as well as the nucleation and growth of Bi_2MoO_6 nanoparticles (Fig. S1C). Increasing the amount further to 2 mmol causes the morphology of the Bi_2MoO_6 nanostructures to change significantly. TNTs are partially coated with Bi_2MoO_6 nanoflowers (Fig. S1D). It appears that the nanoflowers are composed of a number of nanosheets, which radially grow from the center.

On the basis of the integrated area under the CV curve (Fig. S2A), the areal capacitances of BMO/TNT-3, BMO/TNT-5, BMO/TNT-6, and BMO/TNT-7 are 110.3, 90.1, 74.4 and 56.3 mF cm^{-2} at a scan rate of 40 mV s^{-1}, respectively. From the discharging curves (Fig. S2B), the areal capacitances of those samples are 330, 279,

246 and 235 mF cm^{-2} at a current density of 1 mA cm^{-2}. The results show that the BMO/TNT-3 presents better electrochemical performance.

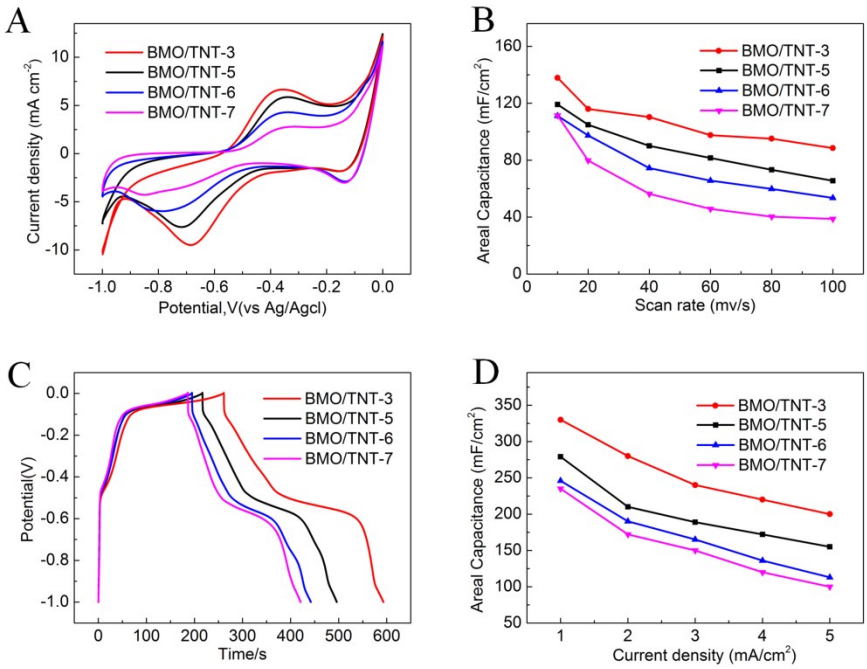

Fig. S2 The CV plots at a scan rate of 40 mV s^{-1} for BMO/TNT-3, BMO/TNT-5, BMO/TNT-6 and BMO/TNT-7 (A), areal capacitances of these samples measured as a function of scan rate (B), The GCD curves at a current density of 1 mA cm^{-2} for BMO/TNT-3, BMO/TNT-5 BMO/TNT-6 and BMO/TNT-7 (C), the average areal capacitance at different current densities (D).

As we all know that the semiconducting nature and poor electrical conductivity of TiO_2 lead to the lower electrochemical activity. From Fig. S3, the areal capacitance of TNTs is only 5.8 mF cm^{-2} at a current density of 1 mA cm^{-2}. Nevertheless, the areal capacitance of BMO/TNT-3 is 330.0 mF cm^{-2} (Fig. S4), ~ 57 times more than the pristine TNTs electrodes.

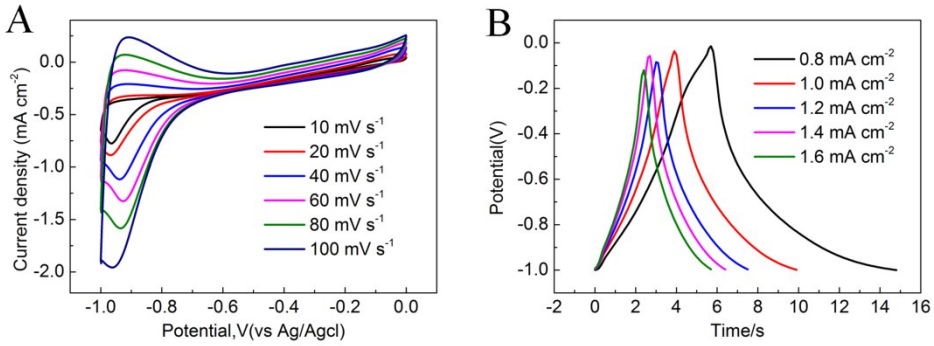

Fig. S3 the CV plots at different scan rates for TNTs (A), galvanostatic charge–discharge curves for TNTs achieved from 0.8 mA cm^{-2} to 1.6 mA cm^{-2} (B).

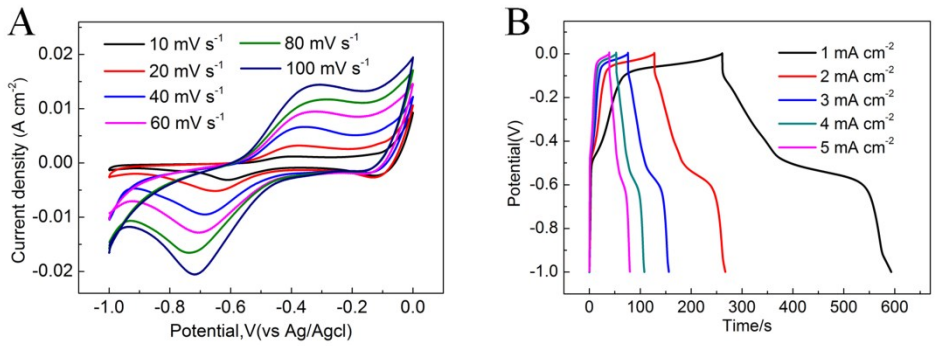

Fig. S4 the CV plots at different scan rates for BMO/TNT-3 (A), galvanostatic charge–discharge curves for BMO/TNT-3 achieved from 1.0 mA cm^{-2} to 5.0 mA cm^{-2} (B).

In the end, by simply tuning the temperature of the solvothermal treatment, while keeping the precursor amount (1.0 mmol $Bi(NO_3)_3 \cdot 5H_2O$ and 0.5 mmol $Na_2MoO_4 \cdot 2H_2O$) and reaction time (12 h) unchanged, the morphology of the Bi_2MoO_6 nanostructures grown on TNTs can be further controlled. The Bi_2MoO_6/TNTs composites prepared at 140℃, 180℃, 200℃ for 12 h were referred as BMO/TNT-8, BMO/TNT-9, BMO/TNT-10, respectively.

Fig. S5B-D shows the SEM images of the BMO/TNT-8, BMO/TNT-9, and BMO/TNT-10, respectively. A lot of Bi_2MoO_6 nanoflakes grow on the surface of TNTs during the solvothermal treatment at 140 ℃. When the temperature increases to 180 ℃, the thin Bi_2MoO_6 nanoflakes are more compact. However, a further increase in the temperature to 200℃ causes the morphology of the Bi_2MoO_6 to present non-uniform distributed nano-block structures.

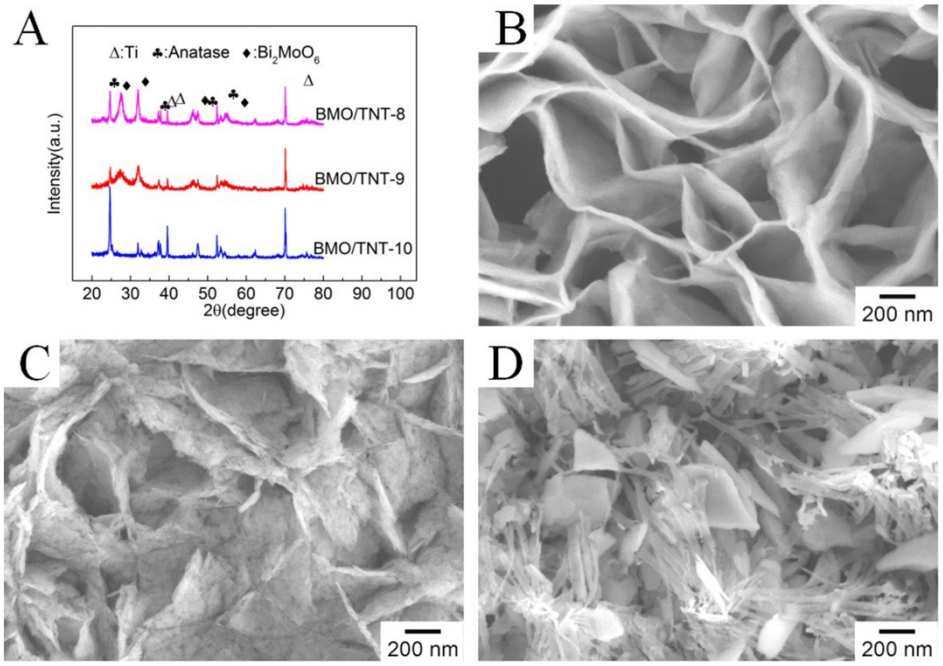

Fig.S5 XRD patterns of the samples BMO/TNT-8, BMO/TNT-9 and BMO/TNT-10 (A). SEM images of BMO/TNT-8 (B), BMO/TNT-9 (C), BMO/TNT-10 (D).

From Fig. S6, the areal capacitances of BMO/TNT-3, BMO/TNT-8, BMO/TNT-9, and BMO/TNT-10 were 330, 265, 245 and 84 mF cm^{-2} at a current density of 1 mA cm^{-2}, respectively. It demonstrates that the proper reaction temperature can be propitious to improve the electrochemical properties of the composite electrode.

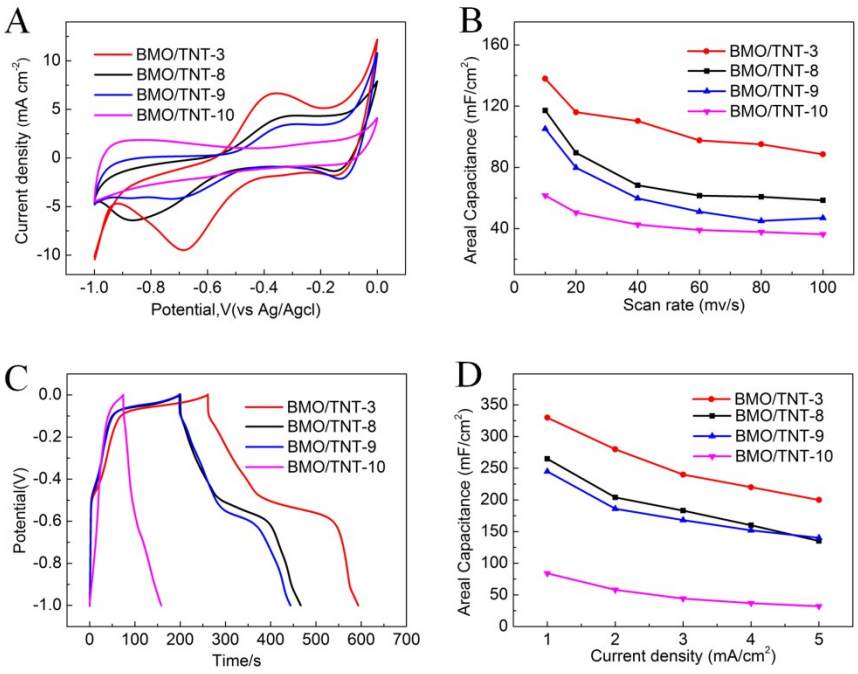

Fig. S6 The CV plots at a scan rate of 40 mV s^{-1} for BMO/TNT-3, BMO/TNT-8, BMO/TNT-9 and BMO/TNT-10 (A), areal capacitances of these samples measured as a function of scan rate (B), The GCD curves at a current density of 1 mA cm^{-2} for BMO/TNT-3, BMO/TNT-8, BMO/TNT-9 and BMO/TNT-10 (C), the average areal capacitance at different current densities (D).

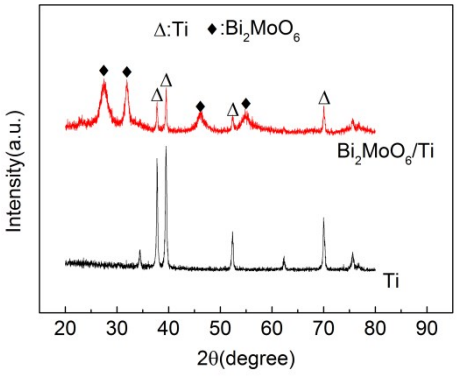

Fig.S7 XRD patterns of the samplesTi and Bi_2MoO_6/Ti.